Published in final edited form as:
Mol Cell Neurosci. 2012 February ; 49(2): 171–183. doi:10.1016/j.mcn.2011.11.007.

PTEN regulates retinal interneuron morphogenesis and synaptic layer formation

Kiyo Sakagami[1], **Bryan Chen**[1], **Steven Nusinowitz**[1], **Hong Wu**[2,3], and **Xian-Jie Yang**[1,3]
[1]Jules Stein Eye Institute, University of California, Los Angeles, CA, USA

[2]Department of Molecular and Medical Pharmacology, University of California, Los Angeles, CA, USA

[3]Molecular Biology Institute, University of California, Los Angeles, CA, USA

Abstract

The lipid phosphatase PTEN is a critical negative regulator of extracellular signal-induced PI3K activities, yet the roles of PTEN in the neural retina remain poorly understood. Here, we investigate the function of PTEN during retinal development. Deletion of *Pten* at the onset of neurogenesis in retinal progenitors results in the reduction of retinal ganglion cells and rod photoreceptors, but increased Müller glial genesis. In addition, PTEN deficiency leads to elevated phosphorylation of Akt, especially in the developing inner plexiform layer, where high levels of PTEN are normally expressed. In *Pten* mutant retinas, various subtypes of amacrine cells show severe dendritic overgrowth, causing specific expansion of the inner plexiform layer. However, the outer plexiform layer remains relatively undisturbed in the *Pten* deficient retina. Physiological analysis detects reduced rod function and augmented oscillatory potentials originating from amacrine cells in *Pten* mutants. Furthermore, deleting *Pten* or elevating Akt activity in individual amacrine cells is sufficient to disrupt dendritic arborization, indicating that *Pten* activity is required cell autonomously to control neuronal morphology. Moreover, inhibiting endogenous Akt activity attenuates inner plexiform layer formation in vitro. Together, these findings demonstrate that suppression of PI3K/Akt signaling by PTEN is crucial for proper neuronal differentiation and normal retinal network formation.

Keywords

Mouse retinal development; PTEN function; retinal specific knockout; PI3K/Akt signaling; amacrine cell morphogenesis

INTRODUCTION

The vertebrate retina is a sophisticated neural network organized into three cellular layers interconnected by two synaptic layers (Sanes and Zipursky, 2010). A common progenitor pool gives rise to seven major retinal cell classes, which can be further classified into more

Corresponding Author: Xian-Jie Yang, Jules Stein Eye Institute, UCLA School of Medicine, 100 Stein Plaza, Los Angeles, CA 90095, USA, Tel 310-825-7020, Fax 310-794-2144, Yang@jsei.ucla.edu.

than 60 subtypes of neurons based on gene expression profiles ad morphologies (Livesey and Cepko, 2001; Masland, 2001). Determination of retinal cell fates is predominantly dictated by cell-intrinsic determinants, especially the combinations of various transcription factors (Hatakeyama and Kageyama, 2004; Ohsawa and Kageyama, 2008). In addition, contact-mediated and secreted signals also influence retinal progenitor proliferation and fate specification (Jadhav et al., 2006; Kim et al., 2005; Sakagami et al., 2009; Wang et al., 2005; Yang, 2004; Yaron et al., 2006; Zhang and Yang, 2001). Upon establishing cellular identities, the morphogenesis of various neurons appears to follow intrinsic differentiation programs (Kay et al., 2004). Recent studies have revealed that retinal cell soma and dendritic arbor distribution involves self-recognition through cell adhesion molecules (Fuerst et al., 2009; Fuerst et al., 2008; Yamagata and Sanes, 2008), while synaptic connection and pruning involve classic immune molecules (Stevens et al., 2007; Xu et al., 2010). Nonetheless, a comprehensive understanding of retinal network formation, especially its modulation by cell extrinsic signals, is still lacking.

The phosphatase and tensin homolog deleted on chromosome 10 (PTEN) has emerged as an important regulator of growth factor signaling in the nervous system (Iwanami et al., 2009). *Pten* encodes a lipid phosphatase that antagonizes the activity of phosphotidylinosital-3-kinase (PI3K), which can be activated by receptor tyrosine kinase (RTK) or G-protein-coupled receptor (GPCR) mediated extracellular signals (Engelman et al., 2006). Inactivating *Pten* elevates the intracellular level of phosphatidylinositol 3,4,5-triphosphate (PIP3) and consequently triggers activation of PDK1 and mammalian target of rapamycin complex 2 (mTORC2) (Manning and Cantley, 2007). Both PDK1 and mTOR subsequently activate Akt through phosphorylation at distinct sites.

Deletion of *Pten* in the developing mouse brain leads to over-proliferation of progenitors and enhanced neuronal survival (Backman et al., 2001; Groszer et al., 2001; Kwon et al., 2001). *Pten* null neural progenitor cells show reduced growth factor dependency, shortened cell cycles and accelerated G0–G1 entry (Groszer et al., 2006). *Pten* mutation-induced Akt activation also leads to hypertrophic neuronal somata and more elaborate dendritic arbors of cortical neurons (Jaworski et al., 2005; Kwon et al., 2006). In the adult nervous system, deletion of *Pten* enhances neurogenesis through perpetual self-renewal of endogenous stem cells (Gregorian et al., 2009). Inactivation of *Pten* also activates mTOR and promotes axonal regeneration of CNS neurons (Liu et al., 2010; Park et al., 2008).

In the developing eye, ablation of *Pten* in the retinal pigment epithelium (RPE) causes the loss of adhesion junctions, an epithelial to mesenchymal transition, abnormal RPE cell migration, and ultimately the death of adjacent photoreceptor cells (Kim et al., 2008). In the mature retina, activation of the insulin/mTOR pathway has been shown to delay cone photoreceptor death in mouse models of retinitis pigmentosa (Punzo et al., 2009). However, the function of PTEN during development of the neural retina has not been elucidated. In this study, we have abolished PTEN function from the onset of retinal neurogenesis. We provide evidence that PTEN activity differentially influences retinal neuron production and critically regulates retinal synaptic layer formation. We further demonstrate that PTEN acts cell-autonomously to suppress PI3K/Akt activation and control amacrine interneuron morphogenesis.

MATERIALS AND METHODS

Mice

The *Pten* floxed mouse line was previously described (Groszer et al., 2001). The Chx10-cre transgenic mouse line was generated by Rowan and Cepko (Rowan and Cepko, 2004). Both mouse lines were backcrossed for more than six generations to the C57Bl6 background.

Pten conditional mutant (*Pten* $^{fl/fl}$*; Chx10-cre, Pten* cKO) and littermate control (*Pten* $^{fl/fl}$) were used for analyses. All animal procedures were approved by the Animal Research Committee at University of California, Los Angeles.

Histology and Golgi Staining

Eye cups without lenses or whole heads (P0) were fixed in 4% paraformaldehyde (PFA)/phosphate buffered saline (PBS) for one hour to overnight at 4°C. For paraffin sections, fixed samples were dehydrated through graded ethanol and 100% xylene series, and embedded in paraffin wax. Paraffin sections of 8 μm thickness were collected. Standard Hematoxylin and Eosin staining was performed using dewaxed paraffin sections.

A modified Golgi staining method based on Pilati et al. (Pilati et al., 2008) was used. P45 mouse retinas were dissected in 4% PFA/10mM HEPES/distilled H_2O (dH_2O) at pH 5.8 or 7.4 and immersed in fixative chromation buffer (3% potassium dichromate/2% glutaraldehyde/0.25% osmium tetroxide/dH_2O at pH 5.8 or 7.4) for 48 hours at room temperature in the dark. After chromation, tissues were rinsed with 0.75% silver nitrate/dH_2O several times and immersed in 2% silver nitrate/dH_2O for 48 hours at room temperature in the dark. After cryoprotection in 30% sucrose/dH_2O, retinas were embedded in OCT compound and immediately frozen. Sections 50 μm in thickness were counterstained with 0.1% cresyl violet (Sigma)/dH_2O for 5 min and rinsed with dH_2O. Retinal sections were dehydrated in graded ethanol, cleared in xylene, and mounted in paramount (Fisher Scientific).

Immunohistochemistry and Imaging

Immunohistochemistry was performed as previously described (Sakagami et al., 2009). For whole mount labeling, the orientation of the eyes was demarcated before dissection and fixed in 4% PFA/PBS overnight at 4°C. Retinal sections were incubated with the following primary antibodies against: PTEN (138G6, Cell Signaling, #9559, 1:100), GFP (Molecular Probes, A11122, 1:500), phospho-Akt (Ser473) (D9E, Cell signaling, #460S, 1:100), Brn3a (Chemicon, MAB1585, 1:100), type III β-Tubulin (TUJ1, Covance, RBP-435P, 1:1000), Pax6 (Chemicon, AB5409, 1:1000), AP-2α (3B5, Developmental Studies Hybridoma Bank, 1:2), Chx10 (Chemicon, AB9014, 1:100), Protein Kinase C alpha (PKCα)(Santa Cruz, MC5, sc-80, 1:100), Prox1 (Chemicon, AB5475, 1:1000), Glutamine Synthetase (GS)(Chemicon, MAB302, 1:500), Recoverin (Chemicon, AB5585, 1:5000), Rhodopsin (Rho4D2, kindly provided by Dr. R. Molday,1:320), M-opsin (Chemicon, AB5405, 1:200), S-opsin (Chemicon, AB5407, 1:200), Syntaxin (HPC-1, Sigma, S-0664, 1:200), Glutamate Decarboxylase 65 (GAD65)(Chemicon, AB5082 1:200), Glycine Transporter (GlyT)1 (Chemicon, AB1770, 1:5000), Calbindin D-28K (Chemicon, AB1778, 1:500), Choline Acetyltransferase (ChAT)(Chemicon, AB144P, 1:100), Synaptophysin (SIGMA, S5768, 1:200), Bassoon (SAP7F407, Stressgen, VAM-PS003, 1:100), Pax6 (Millipore, AB5409, 1:1000), PCNA (Sigma, P3825, 1:2000), Caspase3 (R&D, AF835, 1:2000), BrdU (Amersham, PRN202). Secondary antibodies conjugated with Alexa 488 or Alexa 568 (Molecular Probes, 1:500) were used with 10mg/ml 4′, 6-diamidino-2-phenylindole (DAPI; Roche). Immunofluorescent images were captured using a Nikon E800 microscope equipped with a SPOT digital camera or laser scanning confocal microscopes (Leica TCS-SP, or Olympus BX61 and Fluoview1000). For confocal imaging of flat mount retinas, the tissues were scanned in 100 μm depth from the RGC side with 1μm step size. The numbers of ChAT-positive cells in 160 μm x160 μm x100 μm scanned tissue volume were quantified.

Flow Cytometry

Flow cytometry was performed as previously described (Sakagami et al., 2009). Dissociated cells fixed in 0.25% PFA/PBS were incubated with the following primary antibodies

against: Brn3a, AP2a, Chx10, Cyclin (Cyc) D3 (DCS22, Cell Signaling, 1:100) and pan-Brn3 (C-13, Santa Cruz, sc-6026, 1:20). Cells were incubated with 10 mg/ml DAPI and Alexa-488 or Alexa-647 conjugated secondary antibodies (Molecular Probes, 1:500). Flow cytometry was performed using an LSR flowcytometer (BD Biosciences) and analyzed with Cell Quest (BD) and Modfit (BD) software. A minimum of 30,000 cells was analyzed for each sample.

Western Blotting

Western Blotting was performed as previously described (Rhee et al., 2004). Pairs of retina at P0 or P13 were dissected in HBSS and lysed in RIPA-solution containing proteinase inhibitors, 100mg/ml Aprotinin, 100mg/ml Leupeptin and 1mg/ml Pepstatin A. Retinal extracts (20mg) were subjected to Western blot analyses using primary antibodies against: PTEN (138G6, Cell Signaling, #9559, 1:1000), Akt1 (C73H10, Cell Signaling, #2938S, 1:1000), phospho-Akt (Ser473; D9E)(Cell signaling, #4060S, 1:2000), and acetylated Tubulin (α-Tubulin, 6-11B-1) (SIGMA, T7451, 1:4000). Secondary antibodies conjugated with HRP (Amersham Biosciences, NA931V or NA934V, 1:1500) were detected with Enhanced Chemiluminescence System (Amersham Biosciences, RPN2132).

DNA Constructs and in vivo Electroporation

Electroporation was performed according to an established procedure (Matsuda and Cepko, 2004). For *Pten* deletion in individual cells, a mixture of the DNA vector LIA (Fields-Berry et al., 1992) and plasmids encoding the CAG promoter (Niwa et al., 1991) upstream of either GFP (CAG-GFP) or cre-GFP (CAG-cre-GFP) at 5 mg/ml was co-injected into the subretinal space of P0 homozygous *Pten* floxed mice. Animals were harvested at P21 and analyzed by alkaline phosphatase histochemistry (Fields-Berry et al., 1992). To test effects of Akt activation, we subcloned a myristorylated form of mouse Akt1 (Zhou et al., 2000) or GFP downstream of the CAG promoter (Niwa eta al., 1991). Mixtures of the CAG-GFP plasmid with either pCAG mock or pCAG-ca.Akt were electroporated into P0 wild type mouse retinas. Eyes were harvested and analyzed by anti-GFP Immunolabeling at P21.

Explant culture

P0 retinas were dissected and placed with the ganglion cell side up on top of transwell filter inserts (Millipore, Millicell PICMORG50) in the culture medium (44% HAM'S F-12 (SAFC Bioscience, 51651C)/44% DMEM (SAFC Bioscience, 51441C)/10% FCS (Hyclone)/1% N2 supplement (GIBCO, 17502048)/1% Penicillin and Streptomycin (GIBCO, 15140)). The Akt inhibitor (EMD Chemicals, 124005)(Hu et al., 2000) was dissolved in DMSO (Sigma, D2650) and added to a final concentration of 10 μM in 0.1% of DMSO from the beginning of the culture. The controls were exposed to 0.1% DMSO alone. The medium was changed every other day, and retinas were cultured for 8 days at 37°C with 5% CO_2.

Electroretinogram (ERG)

ERGs were recorded as previously described (Heckenlively and Arden, 1991; Nusinowitz and Heckenlively, 2006). Briefly, after overnight dark-adaptation, ERGs were recorded from the corneal surface of the eye. All stimuli were presented in a large integrating sphere coated with highly reflective white matte paint (#6080, Eastman Kodak Corporation, Rochester, NY). A photic stimulator (Model PS33 Plus; Grass-Telefactor, West Warwick, RI) affixed to the outside of the sphere illuminated its interior with brief flashes of light. Responses were amplified 10,000 × (Grass P511 High Performance AC Amplifier), band-pass filtered (0.1–300 Hz), digitized using an I/O board (PCI-6221, National Instruments, Austin, TX) in a personal computer, and averaged. Rod-mediated responses were recorded to blue flashes

(Wratten 47A; λ_{max} = 470 nm) varied over an intensity range of 4.0 log-units up to the maximum allowed by the photic stimulator. Cone-mediated responses were obtained with white flashes on a rod-saturating background (32 cd/m^2). All stimuli were presented at 1 Hz except for the brightest flashes where the presentation rate was slowed to 0.2 Hz. To extract oscillatory potentials (Heynen et al., 1985; Wachtmeister, 1998), signals recorded to the brightest flashes were band-pass filtered between 50 Hz to 170 Hz.

Statistical Analyses

Data were expressed as mean ± SD. Pairwise comparisons were performed using Student's t-test.

RESULTS

PTEN Negatively Regulates Akt Signaling in the Developing Retina

To investigate the potential role of PTEN in retinal development, we performed retina-specific *Pten* gene ablation using cre-*loxP* homologous recombination. Mice carrying the *Pten* floxed allele (*Pten*^{fl}) (Groszer et al., 2001) were crossed with *Chx10-cre* driver mice, which express a cre-GFP fusion protein in retinal progenitor cells starting at embryonic day 11 (E11) (Rowan and Cepko, 2004). As observed previously (Sakagami et al., 2009), cre-GFP was detected in the majority of retinal progenitor cells residing in the ventricular zone (VZ) at postnatal day 0 (data not shown), indicating that most retinal cells had been exposed to the cre activity.

We first examined the expression patterns of PTEN protein in the developing and mature retina using immunocytochemistry. In the P0 control retina (*Pten* $^{fl/fl}$, no cre), strong PTEN immunolabeling signals were present in the inner retina coinciding with postmitotic RGCs and amacrine cells; while weaker PTEN signals were detected in the VZ occupied by postnatal progenitors and prenatally produced photoreceptor and horizontal cell precursors (Fig. 1A). By P18, when the control retina approached maturity, PTEN protein became broadly distributed in the inner plexiform layer and the ganglion cell layer, and was expressed at a low level in the inner nuclear layer (Fig. 1C). In the P0 *Pten* cKO retinas, PTEN protein signals were abolished in the ventricular zone and diminished in the inner retina (Fig. 1B). The P18 *Pten* cKO retina also lost most PTEN expression, with the exception of a few scattered cells (Fig. 1D), which likely reflected the varying degree of *Chx10-cre* mosaicism (Rowan and Cepko, 2004; Sakagami et al., 2009). Western blot analysis further confirmed the reduction of PTEN protein in *Pten* cKO retinas (Fig. 1K).

We next tested whether *Pten* deletion altered Akt expression or activation in the retina. Immunofluorescent labeling did not detect changes of total Akt protein expression between controls and Pten cKO at P18 (Fig. 1I, J). We also analyzed the distribution of the phosphorylated Akt at Serine residue 473. In the control retinas, very low levels of pAkt were detected at P0 (Fig. 1E). In contrast, *Pten* cKO retinas showed elevated Akt phosphorylation, especially in the developing inner plexiform layer (Fig. 1F). In the control P18 retinas, weak pAkt signals were detected in the ganglion cell layer and in the inner nuclear layer (Fig. 1G). In comparison, the P18 *Pten* cKO retina showed significantly elevated pAkt in the inner nuclear layer, ganglion cell layer, and both plexiform layers with the exclusion of the outer nuclear layer (Fig. 1H). Consistently, Western blots showed elevated pAkt in homozygous *Pten* cKO mutant, but not in *Pten* heterozygous retinas (Fig. 1K). These results demonstrate that PTEN plays a key role in regulating Akt phosphorylation during retinogenesis, especially in the developing inner plexiform layer.

Histological analysis further revealed morphological defects caused by the *Pten* deletion (Fig. 1L). The P18 mutant retina had a disorganized and thinner outer nuclear layer

compared to the control. Furthermore, both the inner nuclear layer and the ganglion cell layer were thicker and contained hypertrophic cell somata. In addition, the inner plexiform layer, but not the outer plexiform layer, was dramatically expanded and contained ectopically localized cell somata. Therefore, ablation of *Pten* at the onset of retinogenesis causes severe disruption of normal retinal development.

PTEN Function Differentially Affects Retinal Cell Production and Differentiation

To investigate whether *Pten* deficiency affected production of retinal cell types, we performed retinal cell marker analyses. The early born RGCs were assayed using the POU-homeo domain protein Brn3a, a specific marker for differentiated RGCs. At P0, immunolabeling for Brn3a showed that most RGCs are properly localized to the ganglion cell layer in *Pten* cKO retinas, with the exception of a few ectopic cells (Fig. 2C, D). Immunolabeling of Pax6, normally expressed at high levels in postmitotic amacrine cells and RGCs, also detected ectopic Pax6-positive cells in the VZ at P0 (Fig. 2G, H). In addition, more extensive distribution of the neuronal marker β-Tubulin was detected in the VZ at P0 (Fig. 2E, F). Quantitative FACS analysis for Brn3a-labeling showed a 32.2% reduction of RGCs at P0 (Fig. 2J) and a 45.4% reduction of RGCs at P10 (Fig. 3O). At P18, mislocalization of RGCs was apparent with Brn3a-positive cells scattered throughout the inner half of the *Pten* cKO retina (Fig. 3C, D). In addition, *Pten* mutants contained an increase of Caspase3-positive apoptotic cells in the ganglion cell layer at P18 (Suppl Fig. 2E, F).

We next examined effects of *Pten* deletion on retinal interneuron production. Immunolabeling for the amacrine cell-expressed transcription factor AP2α showed a more dispersed distribution and ectopic localization of AP2α positive cells in the inner plexiform layer at P18 (Fig. 3G, H). The perturbed amacrine cell distribution was further confirmed by immunolabeling of Prox1, a transcription factor expressed by horizontal cells, bipolar cells, and the AII subtype of amacrine cells (Dyer et al., 2003). In the *Pten* cKO mutant, the locations of horizontal cells and bipolar cells were only mildly affected, whereas the Prox1-positive AII amacrine cells, which normally lined the boundary of the inner nuclear layer and the inner plexiform layer, showed severe disruption (Fig. 3E, F). Despite the abnormal amacrine cell localization, quantification of AP2α-positive cells did not detect significant changes at P0 (Fig. 2J) and only a minor increase at P10 from 3.6 % to 4.2 % (Fig. 3O). Characterization of the pan-bipolar marker Chx10 showed that somata of most bipolar interneurons were positioned correctly (Fig. 3I, J) and the total number of bipolar cells was not affected by the *Pten* mutation (Fig. 3O). However, the synaptic terminal zone of PKCα-positive rod bipolar cells was significantly expanded within the inner plexiform layer (Fig. 3M, N).

We also characterized effects of *Pten* deletion on the development of postnatally born Müller glia. Compared to the glutamine synthetase (GS) labeled Müller glia in the control retina, the *Pten* mutant showed more intensely labeled Müller glial termini at the outer limiting membrane near the base of the photoreceptor inner segments (Fig. 3K, L). Quantification of the mature Müller cell marker cyclin D3 showed that in *Pten* cKO mutant retinas Müller glia increased from1.4 % to 3.8 % at P10 (Fig. 3O). Because Müller cells are produced at the end of retinogenesis, we examined if enhanced cell proliferation contributed to the increased gliogenesis. Labeling by the proliferating cell marker PCNA did not detect increased PCNA-positive cells in *Pten* cKO retinas at P8 compared with control retinas (Suppl Fig. 1A, B). Consecutive daily BrdU administration from P25 to P45 also failed to detect persistent cell division in the *Pten* mutant retinas (Suppl Fig. 1C, D). These results suggested that PTEN deficiency could potentially impact postnatal progenitor fate specification.

The retinal specific *Pten* deletion clearly affected photoreceptor cell development and/or survival as revealed by the thinner outer nuclear layer (Fig. 1L). Quantification of cells in the outer nuclear layer indicated that *Pten* cKO retinas had 36.4% reduction of photoreceptor cells at P18 (Fig. 4K). However, photoreceptor-specific Recoverin expression persisted in the entire mutant outer nuclear layer (Fig. 4A, B). Although Rhodopsin immunolabeling revealed that rod photoreceptors were present, they had significantly shortened inner/outer segments in *Pten* cKO retinas (Fig. 4C, D). In addition, *Pten* mutants showed abnormal accumulation of Rhodopsin in the cell body and mislocalization of rod cells to the inner nuclear layer (Fig. 4D, F). In contrast, immunolabeling and quantification of M- and S-opsins indicated that cone photoreceptors were not significantly reduced in number (Fig. 4G–J, K). Nonetheless, abnormal distribution of M-opsin in the outer nuclear layer and outer plexiform layer was detected in the *Pten* mutant (Fig. 4G, H), suggesting possible defects in M-cone differentiation. To examine when the photoreceptor reduction occurred in the *Pten* mutant, we assayed for photoreceptor markers in the early postnatal stages. The *Pten* mutant showed similar Recoverin expression as the controls at P0 (Suppl Fig. 2A, B). In addition, the thicknesses of the outer nuclear layer were similar in the control and *Pten* mutant retinas at P8 when photoreceptor production was mostly complete (Suppl Fig. 2C, D). At P18, *Pten* cKO retinas showed increased Caspase3-positive cells in the outer nuclear layer (Suppl Fig. 2E, F), indicating enhanced apoptosis, which was absence at P8 (data not shown). Thus, *Pten* deletion did not overtly affect the specification and initial differentiation of photoreceptors, but impacted rod morphogenesis and survival.

Together, these results indicate that *Pten* deficiency in the develop retina differentially influences retinal neuronal cell type production, differentiation, and survival.

PTEN Activity Regulates Amacrine Dendritic Development and Proper Laminar Formation

A high level of PTEN protein was expressed in the inner plexiform layer (Fig. 1A) during the period of dendritic development and synaptogenesis (Morgan et al., 2008; Stacy and Wong, 2003). We therefore characterized whether defective morphogenesis of amacrine cells contributed to the expansion of this synaptic layer in the *Pten* cKO mutant. Immunolabeling of the pan amacrine cell marker Syntaxin showed a broader inner plexiform layer in the *Pten* mutant compared to the control retina (Fig. 5A, B), thus confirming the abnormal amacrine morphological development due to the loss of PTEN activity.

To determine the subtypes of amacrine cells affected by the *Pten* mutation, we performed immunolabeling for several amacrine cell markers. The GABAergic and glycinergic amacrine cells represent two major subclasses of amacrine cells. Characterization of GAD65-positive (Fig. 5G, H) and GlyT1-positive (Fig. 5I, J) amacrine cells showed expanded synaptic zones and scrambled sublamina in the *Pten* mutant retina. In addition, somata of Calbindin-positive amacrine cells, which normally occupied both the inner nuclear layer and the ganglion cell layer, were scattered and no longer displayed the two distinct sublaminae in the *Pten* mutant (Fig. 5C, D). In contrast, Calbindin labeling of horizontal cells did not appear affected. Furthermore, the rare TH-positive dopaminergic amacrine cells displayed enlarged cell somata and more elaborate processes across the inner nuclear layer, instead of the restricted extension of neurites along the interface of the inner nuclear layer and the inner plexiform layer (Fig. 5K, L).

We next analyzed the impact of *Pten* deficiency on the distribution and density of the large field cholinergic amacrine cells using confocal imaging on flat mount retinas. In the control retina, somata of ChAT-positive cells were aligned in the ganglion cell layer and inner nuclear layer and their dendrites extended into two synaptic sublaminae in the inner plexiform layer (Fig. 5E, M). In *Pten* cKO mutants, ChAT-positive cells were dispersed in the expanded inner plexiform layer (Fig. 5F, N). Quantification shows that the distance

between any given two ChAT-positive cells in *Pten* cKO is 82.1% farther than in controls (Fig. 5P). Furthermore, the density of ChAT-positive cells in *Pten* cKO retina was 28.3% lower than the control density. Therefore, although the pan amacrine marker AP2α only detected a minor increase of amacrine cells (Fig. 3O), the distribution and number of discrete subtypes of amacrine cells might be influenced by *Pten* cKO.

To further characterize neuronal morphology, we used Golgi staining to visualize arborization of individual cells. P45 control retinas showed a series of amacrine cells with proper somata localization within the inner nuclear layer and relatively narrow dendritic fields (Fig. 6A). In contrast, *Pten* mutant retinas contained numerous ectopic cell somata in the inner plexiform layer (Fig. 6A). Strikingly, *Pten* mutant amacrine cells also displayed more elaborate dendrites and mis-orientated processes (Fig. 6A).

To determine whether PTEN function is required cell autonomously, we generated individual *Pten* mutant cells by expressing cre in *Pten* $^{fl/fl}$ retinas using in vivo electroporation. Control amacrine cells transfected by GFP-expressing plasmid alone exhibited compact dendritic fields (Fig. 6B). In contrast, amacrine cells transfected with the cre-GFP-expressing construct showed broad dendritic arborization (Fig. 6B). Together, these data indicate that PTEN plays a crucial role in regulating dendritic morphologies of most amacrine cells in a cell autonomous manner.

Pten Mutation Disrupts Proper Retinal Function

To determine whether *Pten* deletion disrupted synaptogenesis in addition to dendritic development, we labeled retinal sections for Synaptophysin. In the control, Synaptophysin showed defined expression in both synaptic layers at P18 (Fig. 7A). The *Pten* mutation did not affect the restricted Synaptophysin expression in the outer plexiform layer, but resulted in diffused expression over the expanded inner plexiform layer (Fig. 7B). Similarly, confocal imaging of the presynaptic protein Bassoon showed less intense labeling in the inner plexiform layer (Fig. 7C, C′, D, D′). However, consistent with the inner plexiform layer expansion in *Pten* mutants, Western blots did not detect reduced total Bassoon protein levels (Fig. 7E).

We performed electroretinography (ERG) to evaluate the influence of the *Pten* mutation on retinal function. Under dark-adapted conditions, 12 weeks old *Pten* mutant mice showed mildly to moderately reduced *a*- and *b*- wave amplitudes across all stimulus intensities (Fig. 8). Consistent with the observed reduction of rod photoreceptors (Fig. 4), the *a*-wave of the dark-adapted ERGs showed an approximately 20–25% reduction in amplitude in *Pten* mutants compared to controls (Fig. 8C). The dark-adapted *b*-wave, originating from the retinal interneurons, was similarly reduced (Fig. 8D), likely reflecting the reduced photoreceptor response. The a- to b- wave amplitude ratio was not significantly different between control and *Pten* mutant mice (data not show), suggesting that signal transmission from photoreceptors to downstream cells occurred normally. In contrast, the amplitude of the photopic *b*-wave was not significantly different between the *Pten* mutant and control mice, although there was a trend in the direction of larger cone b-wave amplitudes in *Pten* mice (Fig. 8C, D). This finding is consistent with the mild defects in cone photoreceptors (Fig. 4).

The *Pten* mutant showed larger harmonic components on the edge of the b-wave, which were known as oscillatory potentials (OPs) likely generated by amacrine cells (Wachtmeister, 1998). Under the dark-adapted conditions, the OPs in *Pten* mice were of similar morphology with amplitude and timing parameters not significantly different from control mice (Fig. 8E, F). In contrast, the OPs under photopic conditions appeared more prominent in *Pten* mutant mice (Fig. 8G). While all of the OPs (OP1–OP4) demonstrated

enhanced amplitudes in the *Pten* mutant, only OP2 and OP3 were significantly different from the controls (Fig. 8H). The enhanced inner retina oscillatory potentials correlated with the altered dendritic arbors and changes in synaptic efficacy of amacrine cells involved in the cone-pathway.

Akt Activity Affects Amacrine Cell Morphogenesis

In the *Pten* mutant retina, Akt phosphorylation at Ser473 was significantly elevated in the developing inner plexiform layer (Fig. 1). To determine whether Akt activation is responsible for the observed mutant phenotypes, we electroporated into the wild type P0 retinas a plasmid expressing a constitutively active Akt (ca.Akt), which was myristoylated and thus targeted to the membrane independently of PIP3 triggered activation (Zhou et al, 2000). The control retinas electroporated with CAG-GFP plasmid showed GFP-positive amacrine cells with normal soma positions within the inner nuclear layer and well-defined dendritic arbors (Fig. 9A–C). In comparison, the ca.Akt-expressing plasmid transfected retinas showed GFP-positive cells with more extensive dendritic arbors spreading throughout the inner plexiform layer (Fig. 9D–F). Furthermore, ca.Akt transfected retinas frequently contained GFP-positive amacrine somata ectopically localized within the inner plexiform layer (Fig. 9D–F).

To examine whether endogenous Akt activity regulates normal amacrine cell morphogenesis, we treated wild type P0 retinal explants with an Akt inhibitor (Hu et al., 2000). After 8 days of culture, control retinas without the Akt inhibitor developed two distinct Pax6-positive cell layers segregated by a plexiform layer, similar to normal retinas developed in vivo (Fig. 9G). In contrast, retinal explants exposed to the Akt inhibitor showed collapsed inner plexiform layer and a single layer of Pax6-positive cells (Fig. 9H). Inhibiting endogenous Akt activity also resulted in reduced Syntaxin labeling, reflecting an underdeveloped inner plexiform layer compared to controls (Fig. 9I–J). Furthermore, treatment with the Akt inhibitor resulted in a single row of ChAT-positive somata instead of two rows found in controls (Fig. 9K, L). Moreover, pAkt labeling in the inner plexiform layer was decreased in the retinas cultured in the presence of Akt inhibitor (Fig. 9M, N). Together, these results supported that endogenous Akt activity levels affected the proper morphogenesis of amacrine cells and inner plexiform layer formation.

DISCUSSION

The retina-specific deletion of *Pten* has enabled us to examine the function of PTEN/PI3K signaling during formation of the entire retinal network. Our analyses have revealed essential functions of PTEN in retinal neuron production and differentiation. Furthermore, we demonstrate the critical role of PTEN in controlling dendritic arborization of retinal interneurons within a specific synaptic layer.

Requirements for PTEN/PI3K Signaling in Different Retinal Cell types

During retinogenesis, different levels of growth factor-induced PI3K signaling may influence retinal cell type specification and their subsequent differentiation. Currently, the precise signals activating PI3K in retinal progenitor cells and postmitotic neurons are not fully characterized. However, early born retinal neurons such as RGCs are known to produce multiple growth factors, including RTK-mediated VEGF and neurotrophins, which may influence PI3K activities locally (Hashimoto et al., 2006; Meyer-Franke et al., 1995; Yang and Cepko, 1996). Consistent with the low level of PTEN expressed in progenitor cells, deletion of *Pten* only results in a mild elevation of pAkt among progenitors. In contrast, significant elevation of pAkt occurs in postmitotic neurons in the absence of PTEN, suggesting that PTEN plays important roles in postmitotic retinal neurons. Nonetheless, we

cannot rule out a requirement of PTEN in retinal progenitors. In the *Pten* retinal knockout mutant, although all major retinal cell classes are generated, the proportions of several cell types, including ganglion cells, rod photoreceptors, and Muller glia are altered.

The *Pten* mutation affects both rod and cone photoreceptor development. However, the defect of rod differentiation is more profound. Our analyses indicate that the decreased number of rod photoreceptors in the mature retina is unlikely due to deficits in rod production, since both control and *Pten* mutant retinas show similar numbers of photoreceptor cells at P8. Instead, the main reason for outer nuclear layer thinning in the *Pten* mutant is likely due to increased cell death after P8 as a consequence of defective rod differentiation. Previous reports have shown that mislocalization of rhodopsin in differentiating photoreceptors alone is sufficient to cause rapid cell death (Marszalek et al., 2000). The initial steps regulating photoreceptor fate determination are shared between rod and cone cells (Chen et al., 1997; Furukawa et al., 1997; Nishida et al., 2003), while the subsequent specification of rod versus cone involves different intracellular determinants (Haider et al., 2000; Mears et al., 2001). Further studies are necessary to determine the steps of rod photoreceptor development that are affected by the *Pten* mutation.

The increase in Müller glial cells in *Pten* mutant retinas may be caused by prolonged proliferation of late retinal progenitors. However, our data does not support this notion. Alternatively, a shift of a small number of late progenitors from the rod photoreceptor fate to the glial fate could account for this significant increase in Müller cells. The *Pten* deletion results in elevated pAkt in postnatal progenitor cells, which may bias progenitor cells towards a glial fate. In addition, abnormal photoreceptor cell death or retinal injury results in reactive gliosis (Fisher and Lewis, 2003; Frasson et al., 1999), which is detected in *Pten* mutant retinas. Reactive Müller glial cells are known to secret growth factors such as LIF (Joly S, 2008), a member of the CNTF family of cytokines that promotes Müller glial fate (Goureau et al., 2004) and inhibits rod differentiation (Ezzeddine et al., 1997; Rhee et al., 2004; Rhee and Yang, 2010). Indeed, CNTF has been shown to induce the PI3K/Akt signaling cascade in zebrafish retina (Kassen et al., 2009). It is thus conceivable that *Pten* deficiency induced Akt activation and gliosis may account for the enhanced Müller gliogenesis.

Function of PTEN in Dendritic Development of Amacrine Cells

Previous studies have shown that differentiation of neuronal cells with their characteristic dendritic morphology involves PI3K and Akt signaling (Kumar et al., 2005; Kwon et al., 2006). Moreover, Akt activity regulates growth cone expansion via Rac1 signaling and axonal branching via mTOR in vitro (Grider et al., 2009). In the wild type retina, higher levels of PTEN are expressed in the developing inner plexiform layer where active synaptic connections form among RGCs, bipolar cells, and amacrine interneurons during the first two postnatal weeks (Morgan et al., 2008; Stacy and Wong, 2003).

In the *Pten* cKO retina, all subtypes of amacrine cells examined exhibit overly exuberant and disorganized dendrites. The abnormal formation of amacrine dendrites may be responsible for the mislocalization of cell somata and expansion of the bipolar cell synaptic zone. In the absence of PTEN, we observed a drastic increase of pAkt (Ser473) in the inner plexiform layer. We further demonstrate that elevating Akt activity in individual amacrine cells is sufficient to produce dendritic overgrowth. In addition, depleting endogenous Akt activity in wild type retina results in an underdeveloped inner plexiform layer, presumably due to less elaborate dendrites as revealed by syntaxin labeling. Taken together, these results suggest that phosphorylation of Akt at Ser473 by mTORC2 plays a critical role in proper dendritic development of amacrine cells. In the mouse brain, MyosinV is enriched in growth cones and dendritic spines and is involved in transporting PTEN to different membrane

locations (van Diepen et al., 2009). In addition, the level of PTEN in RGC growth cones is important for axon branching and is tightly regulated by the ubiquitin-proteasome system (Drinjakovic et al., 2010). Similar mechanisms regulating the subcellular localization and the half-life of PTEN may also occur in amacrine cells during active dendritic field formation.

By electroporating a cre-expressing plasmid into *Pten* floxed retinas, we observed that individual *Pten* null amacrine cells develop more elaborate dendritic fields, indicating that PTEN acts cell-autonomously to regulate amacrine cell morphology. We also observed that the distribution of amacrine cell sub-populations differ in *Pten* cKO mutants compared to the control retinas. For example, our data show that the cholinergic amacrine cells are more sparsely distributed in *Pten* mutants. Interestingly, *Pten*-deficient ChAT-positive amacrine cells also display collapsed dendrites in addition to increased cell soma spacing. This is reminiscent of mutant phenotypes observed in the cell adhesion molecules Dscam and Dscam-like (Fuerst et al., 2009; Fuerst et al., 2008; Yamagata and Sanes, 2008). Previous studies have shown that multiple cell intrinsic transcription factors critically regulate fate specification of amacrine subtypes (Cherry et al., 2009; Dullin JP, 2007; Jusuf et al., 2011; Kay et al., 2011; Ohsawa and Kageyama, 2008). For examples, specification of the GABAergic amacrine cells requires the forkhead/winged helix protein Foxn4 to activate basic helix-loop-helix factors Neurod1 and Math3 (Li et al., 2004), whereas the homeodomain proteins Pax6 and Barhl2 are implicated in glycinergic amacrine cell differentiation (Marquardt et al., 2001; Mo et al., 2004). However, it remains unclear how cell extrinsic cues might influence the numbers and distribution of subtypes of amacrine cells to result in a functional network. Our findings suggest that precise levels of PI3K signaling modulated by PTEN in the inner plexiform layer may be involved. Further investigations are necessary to delineate how PTEN/PI3K signaling interfaces with cell intrinsic determinants and cell adhesion molecules to regulate dendritic morphology and spatial distribution of amacrine cells during synaptic layer formation.

Intriguingly, the severe disruption detected in the inner plexiform layer in the *Pten* mutant is less obvious in the outer plexiform layer, where horizontal, bipolar, and photoreceptor cells form synapses. We also observe a much lower level of PTEN expression in the outer plexiform layer compared to the inner plexiform layer. These data imply that distinct extrinsic factors may regulate the morphogenesis of specific neuronal cell types despite common requirements for membrane biogenesis and cytoskeleton reorganization during dendritic development.

Influence of Retinal Function by PTEN mutation

The morphological defects of *Pten* cKO mutants also correlate with visual function deficits. Our scotopic ERG measurement revealed reduced a- and b-wave amplitudes under dark-adapted conditions. This rod-mediated functional deficiency reflects the reduction in rod photoreceptors and their differentiation defects. However, the a- to b- wave amplitude ratio was not significantly different between control and *Pten* cKO mice, suggesting that signal transmission from photoreceptors to downstream cells occurs normally despite significant developmental alterations in the middle retina. Consistent with the mild impact of the *Pten* mutation on cone cells, the photopic ERG assay shows normal a-wave and b-wave parameters.

Among the different subtypes of amacrine interneurons, many make inhibitory synapses with cone bipolar cells (Masland, 2001) and are integral to normal functioning of the primary rod signaling pathway. In *Pten* cKO mutant retinas, AII amacrine cells, which normally couple the cone and rod pathways through gap junction electrical synapses (Dyer et al., 2003; Veruki and Hartveit, 2002), are severely altered. However, we did not observe

selective loss of b-wave amplitude, which would be expected to occur in the absence of AII electrical coupling (Kothmann et al., 2009). Instead, *Pten* cKO mutant mice show augmented OPs that are generated at least in part by amacrine cells, demonstrating enhanced responsiveness under photopic conditions. This result may reflect the enlarged dendritic fields of amacrine cells as revealed by morphological and marker analyses. Our results thus suggest that in addition to the neuronal specific morphogenetic program dictated by cell intrinsic codes (Godinho et al., 2005; Kay et al., 2004), extracellular signal-stimulated PI3K activity may help shape neuronal morphology and the neural network properties of the retina.

PTEN/PI3K in retinal degenerative diseases

Increasing evidence support the crucial roles of PTEN/PI3K signaling in tissue homeostasis and repair. Interestingly, RPE-specific deletion of *Pten* causes photoreceptor degeneration, due to the loss of RPE cells as a consequence of disrupted cell adhesion junctions and an epithelial-to-mesenchymal transition (Kim et al., 2008). The demise of RPE cells due to oxidative stress is a primary cause of age-related macular degeneration (AMD). Thus, RPE-specific *Pten* mutant mice may represent an interesting RPE damage model (Kang et al., 2009). The *Pten* cKO mutant retina consists of defective rods and relatively unaffected cone photoreceptors, and therefore resembles the situation of retinitis pigmentosa, in which rods are defective and die first, followed by cone cell death. A recent study has shown that cone cell survival in several retinitis pigmentosa models is enhanced by insulin-mediated PI3K/mTOR activation (Punzo et al., 2009). Therefore, the *Pten* cKO mice may serve as a useful model to study the relationship between rod and cone degeneration and the signaling events affecting photoreceptor cell survival.

Supplementary Material

Refer to Web version on PubMed Central for supplementary material.

Acknowledgments

We are grateful to Dr. Connie Cepko for generating the Chx10-cre mouse line and Dr. Robert Molday for providing the R4D2 antibody. We thank Michelle Lee, Jennifer Chao, Kendal Kernestin, and Chinatsu Tosha for excellent technical assistance. This work was in part supported by grants from Research to Prevent Blindness Foundation and NIH grants EY12270 and EY019052 to XJY, and NEI core grant P30 EY000331.

References

Backman SA, Stambolic V, Suzuki A, Haight J, Elia A, Pretorius J, Tsao MS, Shannon P, Bolon B, Ivy GO, Mak TW. Deletion of Pten in mouse brain causes seizures, ataxia and defects in soma size resembling Lhermitte-Duclos disease. Nat Genet. 2001; 29:396–403. [PubMed: 11726926]

Chen S, Wang QL, Nie Z, Sun H, Lennon G, Copeland NG, Gilbert DJ, Jenkins NA, Zack DJ. Crx, a novel Otx-like paired-homeodomain protein, binds to and transactivates photoreceptor cell-specific genes. Neuron. 1997; 19:1017–1030. [PubMed: 9390516]

Cherry TJ, Trimarchi JM, Stadler MB, Cepko CL. Development and diversification of retinal amacrine interneurons at single cell resolution. Proc Natl Acad Sci U S A. 2009; 106:9495–9500. [PubMed: 19470466]

Drinjakovic J, Jung H, Campbell DS, Strochlic L, Dwivedy A, Holt CE. E3 ligase Nedd4 promotes axon branching by downregulating PTEN. Neuron. 2010; 65:341–357. [PubMed: 20159448]

Dullin JPLM, Robach M, Henningfeld KA, Parain K, Afelik S, Pieler T, Perron M. Ptf1a triggers GABAergic neuronal cell fates in the retina. BMC Dev Biol. 2007; 7:110. [PubMed: 17910758]

Dyer MA, Livesey FJ, Cepko CL, Oliver G. Prox1 function controls progenitor cell proliferation and horizontal cell genesis in the mammalian retina. Nat Genet. 2003; 34:53–58. [PubMed: 12692551]

Engelman JA, Luo J, Cantley LC. The evolution of phosphatidylinositol 3-kinases as regulators of growth and metabolism. Nat Rev Genet. 2006; 7:606–619. [PubMed: 16847462]

Ezzeddine ZD, Yang X, DeChiara T, Yancopoulos G, Cepko CL. Postmitotic cells fated to become rod photoreceptors can be respecified by CNTF treatment of the retina. Development. 1997; 124:1055–1067. [PubMed: 9056780]

Fields-Berry SC, Halliday AL, Cepko CL. A recombinant retrovirus encoding alkaline phosphatase confirms clonal boundary assignment in lineage analysis of murine retina. Proc Natl Acad Sci U S A. 1992; 89:693–697. [PubMed: 1731342]

Fisher SK, Lewis GP. Müller cell and neuronal remodeling in retinal detachment and reattachment and their potential consequences for visual recovery: a review and reconsideration of recent data. Vision Res. 2003; 43:887–897. [PubMed: 12668058]

Frasson M, Picaud S, Léveillard T, Simonutti M, Mohand-Said S, Dreyfus H, Hicks D, Sabel J. Glial cell line-derived neurotrophic factor induces histologic and functional protection of rod photoreceptors in the rd/rd mouse. Invest Ophthalmol Vis Sci. 1999; 40:2724–2734. [PubMed: 10509671]

Fuerst PG, Bruce F, Tian M, Wei W, Elstrott J, Feller MB, Erskine L, Singer JH, Burgess RW. DSCAM and DSCAML1 function in self-avoidance in multiple cell types in the developing mouse retina. Neuron. 2009; 64:484–497. [PubMed: 19945391]

Fuerst PG, Koizumi A, Masland RH, Burgess RW. Neurite arborization and mosaic spacing in the mouse retina require DSCAM. Nature. 2008; 451:470–474. [PubMed: 18216855]

Furukawa T, Morrow EM, Cepko CL. Crx, a novel otx-like homeobox gene, shows photoreceptor-specific expression and regulates photoreceptor differentiation. Cell. 1997; 91:531–541. [PubMed: 9390562]

Godinho L, Mumm JS, Williams PR, Schroeter EH, Koerber A, Park SW, Leach SD, Wong RO. Targeting of amacrine cell neurites to appropriate synaptic laminae in the developing zebrafish retina. Development. 2005; 132:5069–5079. [PubMed: 16258076]

Goureau O, Rhee KD, Yang XJ. Ciliary neurotrophic factor promotes muller glia differentiation from the postnatal retinal progenitor pool. Dev Neurosci. 2004; 26:359–370. [PubMed: 15855765]

Gregorian C, Nakashima J, Le Belle J, Ohab J, Kim R, Liu A, Smith BK, Groszer M, Garcia DA, Sofroniew VM, Carmichael TS. Pten deletion in adult neural stem/progenitor cells enhances constitutive neurogenesis. J Neurosci. 2009; 11:1874–1886. [PubMed: 19211894]

Grider MH, Park D, Spencer DM, Shine HD. Lipid raft-targeted Akt promotes axonal branching and growth cone expansion via mTOR and Rac1, respectively. J Neurosci Res. 2009; 87:3033–3042. [PubMed: 19530170]

Groszer M, Erickson R, Scripture-Adams DD, Dougherty JD, Le Belle J, Zack JA, Geschwind DH, Liu X, Kornblum HI, Wu H. PTEN negatively regulates neural stem cell self-renewal by modulating G0–G1 cell cycle entry. Proc Natl Acad Sci U S A. 2006; 103:111–116. [PubMed: 16373498]

Groszer M, Erickson R, Scripture-Adams DD, Lesche R, Trumpp A, Zack JA, Kornblum HI, Liu X, Wu H. Negative regulation of neural stem/progenitor cell proliferation by the Pten tumor suppressor gene in vivo. Science. 2001; 294:2186–2189. [PubMed: 11691952]

Haider NB, Jacobson SG, Cideciyan AV, Swiderski R, Streb LM, Searby C, Beck G, Hockey R, Hanna DB, Gorman S, Duhl D, Carmi R, Bennett J, Weleber RG, Fishman GA, Wright AF, Stone EM, Sheffield VC. Mutation of a nuclear receptor gene, NR2E3, causes enhanced S cone syndrome, a disorder of retinal cell fate. Nat Genet. 2000; 24:127–131. [PubMed: 10655056]

Hashimoto T, Zhang XM, Chen BY, Yang XJ. VEGF activates divergent intracellular signaling components to regulate retinal progenitor cell proliferation and neuronal differentiation. Development. 2006; 133:2201–2210. [PubMed: 16672338]

Hatakeyama J, Kageyama R. Retinal cell fate determination and bHLH factors. Semin Cell Dev Biol. 2004; 15:83–89. [PubMed: 15036211]

Heckenlively, RJ.; Arden, BG. Principles and practice of clinical electrophysiology of vision. 1991.

Heynen H, Wachtmeister L, van Norren D. Origin of the oscillatory potentials in the primate retina. Vision Res. 1985; 25:1365–1373. [PubMed: 4090272]

Hu Y, Qiao L, Wang S, Rong SB, Meuillet EJ, Berggren M, Gallegos A, Powis G, Kozikowski AP. 3-(Hydroxymethyl)-bearing phosphatidylinositol ether lipid analogues and carbonate surrogates block PI3-K, Akt, and cancer cell growth. J Med Chem. 2000; 43:3045–3051. [PubMed: 10956212]

Iwanami A, Cloughesy TF, Mischel PS. Striking the balance between PTEN and PDK1: it all depends on the cell context. Genes Dev. 2009; 23:1699–1704. [PubMed: 19651981]

Jadhav AP, Mason HA, Cepko CL. Notch 1 inhibits photoreceptor production in the developing mammalian retina. Development. 2006; 133:913–923. [PubMed: 16452096]

Jaworski J, Spangler S, Seeburg PD, Hoogenraad CC, Sheng M. Control of dendritic arborization by the phosphoinositide-3′-kinase-Akt-mammalian target of rapamycin pathway. J Neurosci. 2005; 7:11300–11312. [PubMed: 16339025]

Joly SLC, Thiersch M, Samardzija M, Grimm C. Leukemia inhibitory factor extends the lifespan of injured photoreceptors in vivo. J Neurosci. 2008; 28:13765–13774. [PubMed: 19091967]

Jusuf PR, Almeida AD, Randlett O, Joubin K, Poggi L, Harris WA. Origin and determination of inhibitory cell lineages in the vertebrate retina. J Neurosci. 2011; 31:2549–2562. [PubMed: 21325522]

Kang KH, Lemke G, Kim JW. The PI3K-PTEN tug-of-war, oxidative stress and retinal degeneration. Trends Mol Med. 2009; 15:191–198. [PubMed: 19380252]

Kassen SC, Thummel R, Campochiaro LA, Harding MJ, Bennett NA, Hyde DR. CNTF induces photoreceptor neuroprotection and Müller glial cell proliferation through two different signaling pathways in the adult zebrafish retina. Exp Eye Res. 2009; 88:1051–1064. [PubMed: 19450453]

Kay JN, Roeser T, Mumm JS, Godinho L, Mrejeru A, Wong RO, Baier H. Transient requirement for ganglion cells during assembly of retinal synaptic layers. Development. 2004; 131:1331–1342. [PubMed: 14973290]

Kay JN, Voinescu PE, Chu MW, Sanes JR. Neurod6 expression defines new retinal amacrine cell subtypes and regulates their fate. Nat Neurosci. 2011; 14:965–972. [PubMed: 21743471]

Kim J, Wu HH, Lander AD, Lyons KM, Matzuk MM, Calof AL. GDF11 controls the timing of progenitor cell competence in developing retina. Science. 2005; 308:1927–1930. [PubMed: 15976303]

Kim JW, Kang KH, Burrola P, Mak TW, Lemke G. Retinal degeneration triggered by inactivation of PTEN in the retinal pigment epithelium. Genes Dev. 2008; 22:3147–3157. [PubMed: 18997061]

Kothmann WW, Massey SC, O'Brien J. Dopamine-stimulated dephosphorylation of connexin 36 mediates AII amacrine cell uncoupling. J Neurosci. 2009; 29:14903–14911. [PubMed: 19940186]

Kumar V, Zhang MX, Swank MW, Kunz J, Wu GY. Regulation of dendritic morphogenesis by Ras-PI3K-Akt-mTOR and Ras-MAPK signaling pathways. J Neurosci. 2005; 25:11288–11299. [PubMed: 16339024]

Kwon CH, Luikart BW, Powell CM, Zhou J, Matheny SA, Zhang W, Li Y, Baker SJ, Parada LF. Pten regulates neuronal arborization and social interaction in mice. Neuron. 2006; 50:377–388. [PubMed: 16675393]

Kwon CH, Zhu X, Zhang J, Knoop LL, Tharp R, Smeyne RJ, Eberhart CG, Burger PC, Baker SJ. Pten regulates neuronal soma size: a mouse model of Lhermitte-Duclos disease. Nat Genet. 2001; 29:404–411. [PubMed: 11726927]

Li S, Mo Z, Yang X, Price SM, Shen MM, Xiang M. Foxn4 controls the genesis of amacrine and horizontal cells by retinal progenitors. Neuron. 2004; 43:795–807. [PubMed: 15363391]

Liu K, Lu Y, Lee KJ, Samara R, Willenberg R, Sears-Kraxberger I, Tedeschi A, Park KK, Jin D, Cai B, Xu B, Connolly L, Steward OBZ, He Z. PTEN deletion enhances the regenerative ability of adult corticospinal neurons. Nature Neurosci. 2010; 13:1075–1081. [PubMed: 20694004]

Livesey FJ, Cepko CL. Vertebrate neural cell-fate determination: lessons from the retina. Nat Rev Neurosci. 2001; 2:109–118. [PubMed: 11252990]

Manning BD, Cantley LC. AKT/PKB signaling: navigating downstream. Cell. 2007; 129:1261–1274. [PubMed: 17604717]

Marquardt T, Ashery-Padan R, Andrejewski N, Scardigli R, Guillemot F, Gruss P. Pax6 is required for the multipotent state of retinal progenitor cells. Cell. 2001; 105:43–55. [PubMed: 11301001]

Marszalek JR, Liu X, Roberts EA, Chui D, Marth JD, Williams DS, Goldstein LS. Genetic evidence for selective transport of opsin and arrestin by kinesin-II in mammalian photoreceptors. Cell. 2000; 102:175–187. [PubMed: 10943838]

Masland RH. The fundamental plan of the retina. Nat Neurosci. 2001; 4:877–886. [PubMed: 11528418]

Matsuda T, Cepko CL. Electroporation and RNA interference in the rodent retina in vivo and in vitro. Proc Natl Acad Sci U S A. 2004; 101:16–22. [PubMed: 14603031]

Mears AJ, Kondo M, Swain PK, Takada Y, Bush RA, Saunders TL, Sieving PA, Swaroop A. Nrl is required for rod photoreceptor development. Nat Genet. 2001; 29:447–452. [PubMed: 11694879]

Meyer-Franke A, Kaplan MR, Pfrieger FW, Barres BA. Characterization of the signaling interactions that promote the survival and growth of developing retinal ganglion cells in culture. Neuron. 1995; 15:805–819. [PubMed: 7576630]

Mo Z, Li S, Yang X, Xiang M. Role of the Barhl2 homeobox gene in the specification of glycinergic amacrine cells. Development. 2004; 131:1607–1618. [PubMed: 14998930]

Morgan JL, Schubert T, Wong RO. Developmental patterning of glutamatergic synapses onto retinal ganglion cells. Neural Dev. 2008; 3:8. [PubMed: 18366789]

Nishida A, Furukawa A, Koike C, Tano Y, Aizawa S, Matsuo I, Furukawa T. Otx2 homeobox gene controls retinal photoreceptor cell fate and pineal gland development. Nat Neurosci. 2003; 6:1255–1263. [PubMed: 14625556]

Niwa H, Yamamura K, Miyazaki J. Efficient selection for high-expression transfectants with a novel eukaryotic vector. Gene. 1991; 108:193–199. [PubMed: 1660837]

Nusinowitz, S.; Heckenlively, RJ. Principles and Practice of Clinical Electrophysiology of Vision. 2. The MIT press; 2006. Evaluating Retinal Function in the Mouse Retina with the Electroretinogram; p. 899-909.

Ohsawa R, Kageyama R. Regulation of retinal cell fate specification by multiple transcription factors. Brain Res. 2008; 1192:90–98. [PubMed: 17488643]

Park KK, Liu K, Hu Y, Smith DP, Wang C, Cai B, Xu B, Connolly L, Kramvis I, Sahin M, He Z. Promoting axon regeneration in the adult CNS by modulation of the PTEN/mTOR pathway. Science. 2008; 322:963–966. [PubMed: 18988856]

Pilati N, Barker M, Panteleimonitis S, Donga R, Hamann M. A rapid method combining Golgi and Nissl staining to study neuronal morphology and cytoarchitecture. J Histochem Cytochem. 2008; 56:539–550. [PubMed: 18285350]

Punzo C, Kornacker K, Cepko CL. Stimulation of the insulin/mTOR pathway delays cone death in a mouse model of retinitis pigmentosa. Nat Neurosci. 2009; 12:44–52. [PubMed: 19060896]

Rhee KD, Goureau O, Chen S, Yang XJ. Cytokine-induced activation of signal transducer and activator of transcription in photoreceptor precursors regulates rod differentiation in the developing mouse retina. J Neurosci. 2004; 24:9779–9788. [PubMed: 15525763]

Rhee KD, Yang XJ. Function and mechanism of CNTF/LIF signaling in retinogenesis. Adv Exp Med Biol. 2010; 664:647–654. [PubMed: 20238069]

Rowan S, Cepko CL. Genetic analysis of the homeodomain transcription factor Chx10 in the retina using a novel multifunctional BAC transgenic mouse reporter. Dev Biol. 2004; 271:388–402. [PubMed: 15223342]

Sakagami K, Gan L, Yang XJ. Distinct effects of Hedgehog signaling on neuronal fate specification and cell cycle progression in the embryonic mouse retina. J Neurosci. 2009; 29:6932–6944. [PubMed: 19474320]

Sanes JR, Zipursky SL. Design principles of insect and vertebrate visual systems. Neuron. 2010; 66:15–36. [PubMed: 20399726]

Stacy RC, Wong RO. Developmental relationship between cholinergic amacrine cell processes and ganglion cell dendrites of the mouse retina. J Comp Neurol. 2003; 456:154–166. [PubMed: 12509872]

Stevens B, Allen NJ, Vazquez LE, Howell GR, Christopherson KS, Nouri N, Micheva KD, Mehalow AK, Huberman AD, Stafford B, Sher A, Litke AM, Lambris JD, Smith SJ, John SW, Barres BA. The classical complement cascade mediates CNS synapse elimination. Cell. 2007; 131:1164–1178. [PubMed: 18083105]

van Diepen TM, Parsons M, Downes PC, Leslie RN, Hindges R, Eickholt JB. MyosinV controls PTEN function and neuronal cell size. Nature Cell Biol. 2009; 11:1191–1196. [PubMed: 19767745]

Veruki ML, Hartveit E. AII (Rod) amacrine cells form a network of electrically coupled interneurons in the mammalian retina. Neuron. 2002; 33:935–946. [PubMed: 11906699]

Wachtmeister L. Oscillatory potentials in the retina: what do they reveal. Prog Retin Eye Res. 1998; 17:485–521. [PubMed: 9777648]

Wang Y, Dakubo GD, Thurig S, Mazerolle CJ, Wallace VA. Retinal ganglion cell-derived sonic hedgehog locally controls proliferation and the timing of RGC development in the embryonic mouse retina. Development. 2005; 132:5103–5113. [PubMed: 16236765]

Xu HP, Chen H, Ding Q, Xie ZH, Chen L, Diao L, Wang P, Gan L, Crair MC, Tian N. The immune protein CD3zeta is required for normal development of neural circuits in the retina. Neuron. 2010; 65:503–515. [PubMed: 20188655]

Yamagata M, Sanes JR. Dscam and Sidekick proteins direct lamina-specific synaptic connections in vertebrate retina. Nature. 2008; 451:465–469. [PubMed: 18216854]

Yang XJ. Roles of cell-extrinsic growth factors in vertebrate eye pattern formation and retinogenesis. Semin Cell Dev Biol. 2004; 15:91–103. [PubMed: 15036212]

Yang XJ, Cepko CL. Flk-1, a receptor for vascular endothelial growth factor (VEGF), is expressed by retinal progenitor cells. J Neurosci. 1996; 16:6089–6099. [PubMed: 8815891]

Yaron O, Farhy C, Marquardt T, Applebury M, Ashery-Padan R. Notch1 functions to suppress cone-photoreceptor fate specification in the developing mouse retina. Development. 2006; 133:1367–1378. [PubMed: 16510501]

Zhang XM, Yang XJ. Regulation of retinal ganglion cell production by Sonic hedgehog. Development. 2001; 128:943–957. [PubMed: 11222148]

Zhou BP, Hu MC, Miller SA, Yu Z, Xia W, Lin SY, Hung MC. HER-2/neu blocks tumor necrosis factor-induced apoptosis via the Akt/NF-kappaB pathway. J Biol Chem. 2000; 275:8027–8031. [PubMed: 10713122]

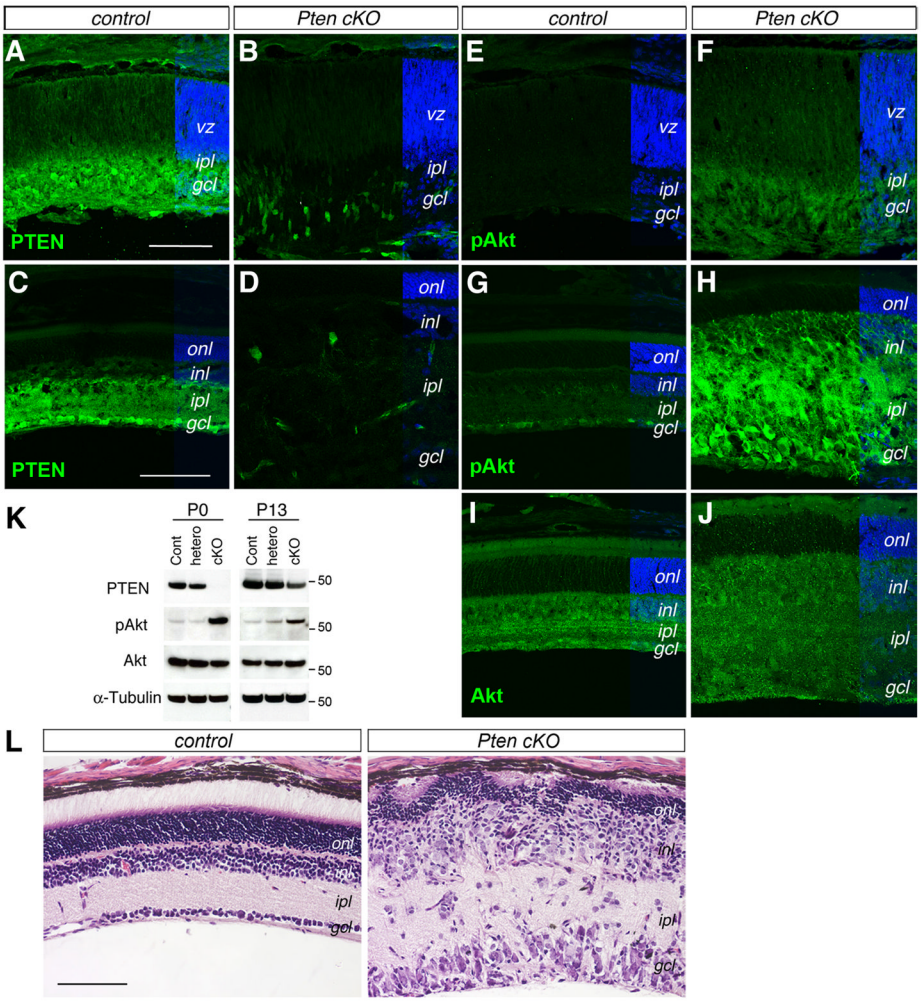

Figure 1. Conditional deletion of Pten enhances Akt phosphorylation and disrupts retinal differentiation

(A–J) Immunolabeling of control (A, C, E, G, I) and *Pten* cKO mutant (B, D, F, H, J) retinas at P0 (A, B, E, F) and P18 (C, D, G–J) for PTEN (A–D), pAkt (E–H), and Akt (I, J). *Pten* cKO retinas show reduced PTEN and increased p-Akt expression.

(K) Western blot analysis of PTEN, p-Akt (Ser473), total Akt, and α-Tubulin in P0 and P13 retinal extracts. MW markers (for 50 kD) are indicated on the right of the panels. (L) H&E staining of control and *Pten* cKO retinas at P18. Note that the *Pten* mutant retina shows a thinner outer nuclear layer and significantly expanded inner retina. *gcl*, ganglion cell layer; *inl*, inner nuclear layer; *ipl*, inner plexiform layer; *onl*, outer nuclear layer; *vz*, ventricular zone. Scale bars, A for (A, B, E, F), C for (C, D, G–J), L, 100 μm.

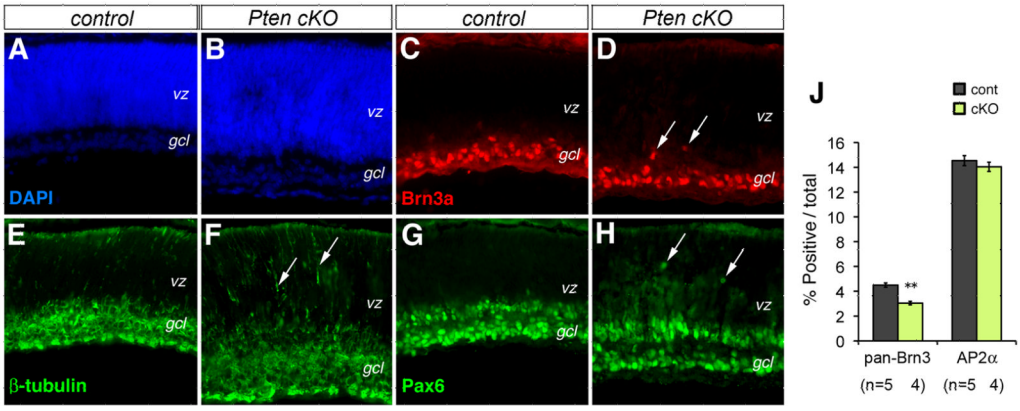

Figure 2. Pten conditional deletion affects retinal cell migration

(A–H) Immunolabeling of control (A, C, E, G) and *Pten* cKO (B, D, F, H) retinas at P0 for neuronal markers Brn3a (C, D), β-Tubulin (E, F), and Pax6 (G, H). Arrows point to mislocalized cells.

(J) Quantification of RGCs and amacrine cells by FACS at P0. Percentages of marker-positive cells among total cells are shown (Individual eyes (n) are indicated below the bar graph. Mean ± S.E.M. **, $p<0.01$).

gcl, ganglion cell layer; *vz*, *ventricular zone*. Scale bar, A for (A–H), 100 μm.

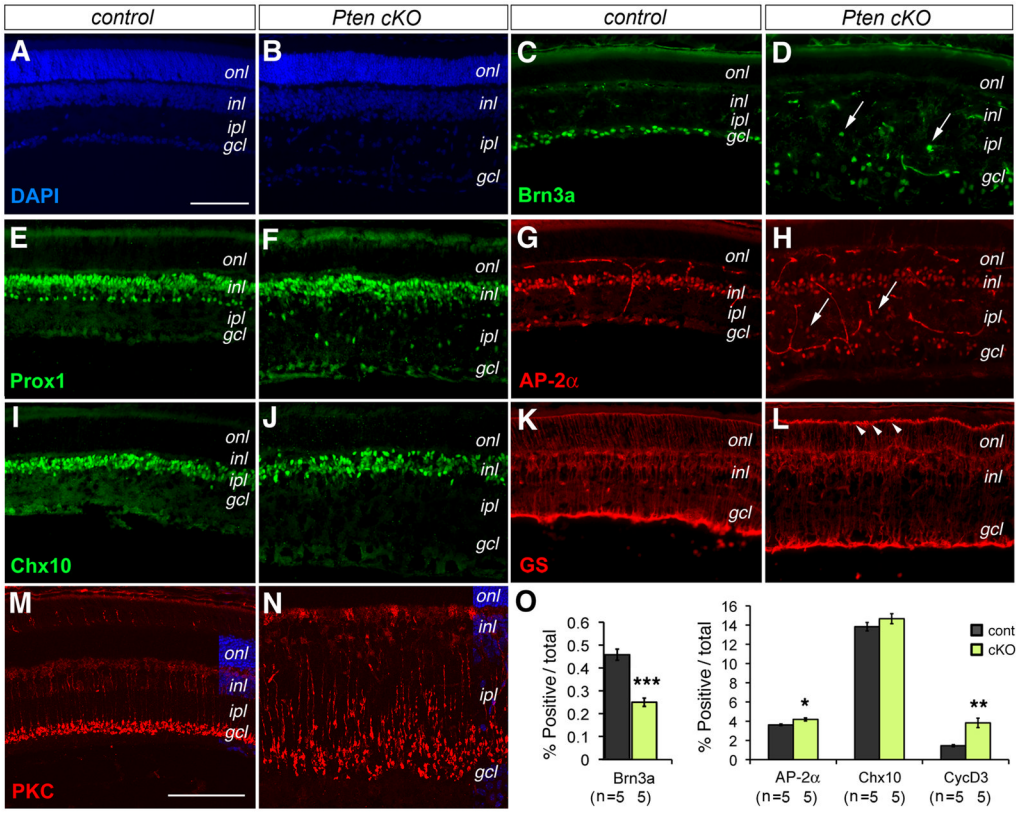

Figure 3. Pten deficiency affects production of neuronal cell types

(A–N) Immunolabeling of control (A, C, E, G, I, K, M) and *Pten* cKO mutant (B, D, F, H, J, L, N) retinas at P18 for neuronal markers Brn3a (C, D, RGCs), Prox1 (E, F, horizontal, bipolar, and AII amacrine cells), AP2α (G, H, amacrine cells), Chx10 (I, J, bipolar cells), GS (K, L, Müller glia), and PKCα (M, N, rod bipolar cells, confocal images). Arrows indicate mislocalized cells. Arrowheads point to intensified outer limiting membrane (L). *gcl*, ganglion cell layer; *inl*, inner nuclear layer; *ipl*, inner plexiform layer; *onl*, outer nuclear layer. Scale bars, A for (A–L), M for (M–N), 100 μm.

(O) Quantification of marker-positive cells among total cells by FACS at P10. A significant reduction in RGCs and increases in amacrine cells and Müller glia are detected (Individual retinas (n) analyzed are indicated. Mean ± S.E.M. ***, $p<0.001$; **, $p<0.01$; *, $p<0.05$).

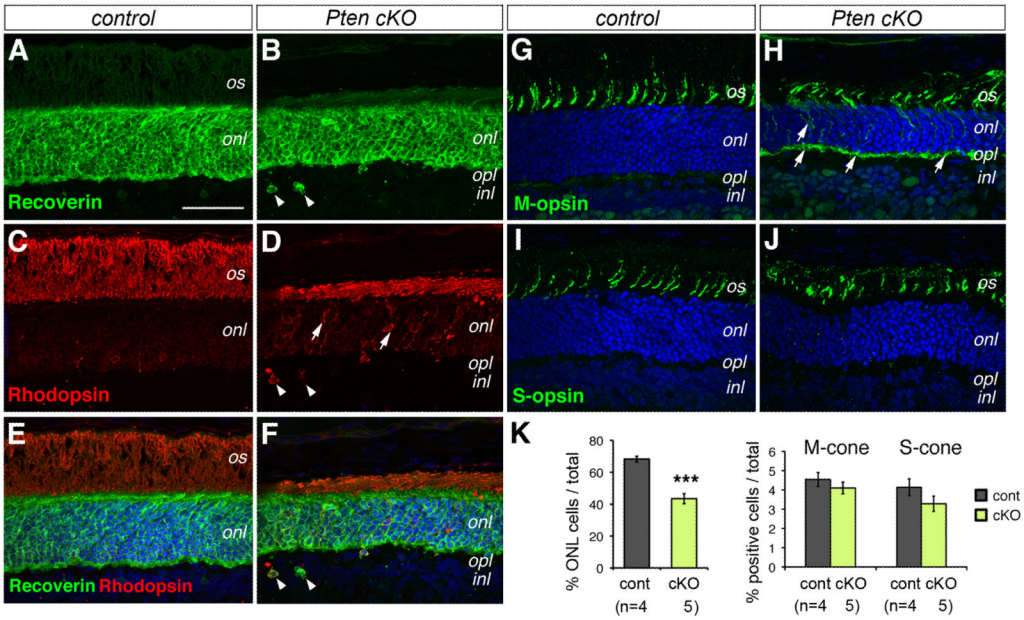

Figure 4. Pten deletion affects rod photoreceptor production and differentiation

(A–J) Confocal fluorescent images of immunolabeled control (A, C, E, G, I) and *Pten* cKO (B, D, F, H, J) retinas at P18 with photoreceptor-specific antibodies. (E, F) are merged images of DAPI with Recoverin (A, B) and Rhodopsin (C, D), respectively. (G–J) are merged images of DAPI and M-opsin (G, H) or S-opsin (I, J). Arrows indicate mislocalized rhodopsin (D) or M-opsin (H). Arrowheads point to ectopic rod photoreceptor cells (D, F). *inl*, inner nuclear layer; *is*, inner segment; *onl*, outer nuclear layer; *opl*, outer plexiform layer; *os*, outer segment. Scale bar, A for (A–J), 100 μm.

(K) Quantification of photoreceptor cells at P18 using confocal microscopy. Percentages of DAPI-labeled outer nuclear layer (ONL) cells or opsin-positive cells among total cells per unit length retina are shown (Individual retinas analyzed (n) are indicated below the bar graph. Mean ± S.E.M. ***, $p<0.001$).

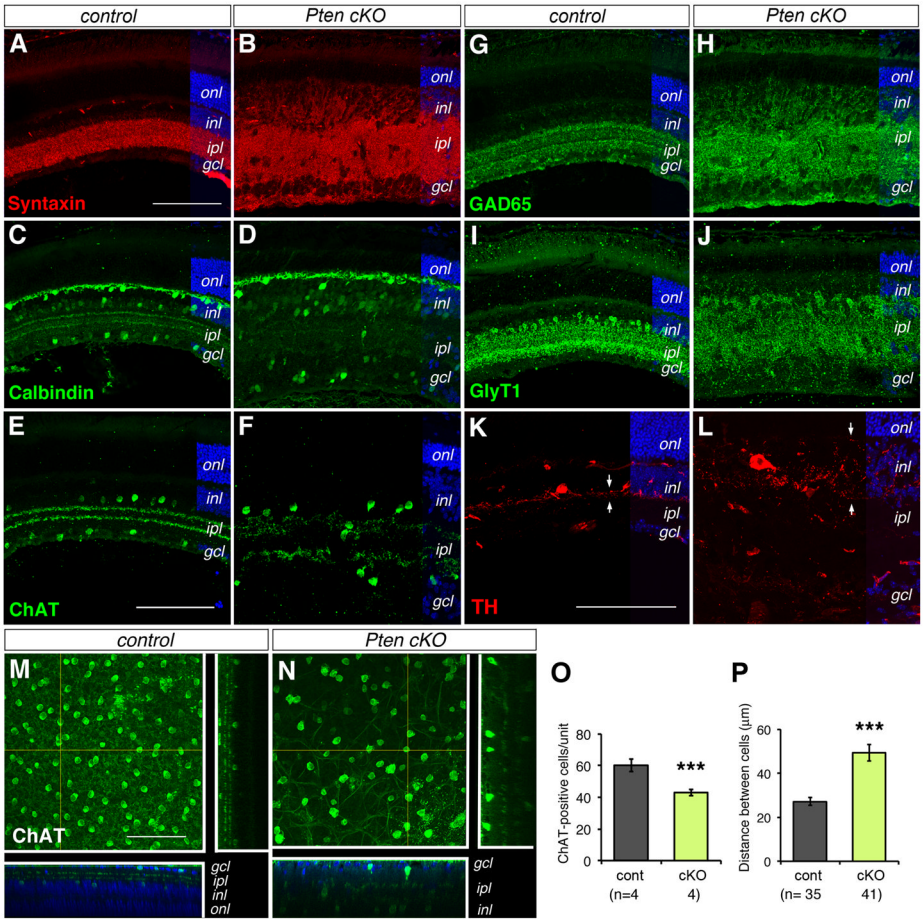

Figure 5. Pten deletion disrupts amacrine morphogenesis and inner plexiform layer formation

(A–L) Confocal fluorescent images of immunolabeled control (A, C, E, G, I, K) and *Pten* cKO (B, D, F, H, J, L) retinas at P18 with amacrine cell markers. Note the expansion of inner plexiform layer indicated by Syntaxin (A, B, pan amacrine cell marker) and the loss of sublaminar stratification revealed by Calbindin (C, D, subset of amacrine cells), ChAT (E, F, cholinergic amacrine cells), GAD65 (G, H, GABAergic amacrine cells), GlyT1 (I, J, glycinergic amacrine cells), and TH (K, L, dopaminergic amacrine cells). Arrows in (K, L) indicate the spread of TH neuritis.

(M, N) Confocal fluorescent images of flat mount control (M) and *Pten* cKO (N) retinas immunolabeled for ChAT at P25. The square panels represent merged confocal optical sections (100 μm). The side and bottom panels show DAPI and ChAT colabeled vertical and horizontal optical sections (1 μm) as indicated by the yellow lines.

gcl, ganglion cell layer; *inl*, inner nuclear layer; *ipl*, inner plexiform layer; *onl*, outer nuclear layer. Scale bars, A for (A, B, C, D, G, H, I, J), E for (E, F), K for (K, L), M for (M, N) 100 μm.

(O, P) Quantification of density and spacing of cholinergic amacrine cells at P25. The numbers of ChAT-positive cells per unit volume and individual retinas (n) analyzed are shown in (O). The distances between any given two ChAT-positive cells and individual cells analyzed (n) are indicated in (P). Mean ± S.E.M. ***, $p<0.001$.

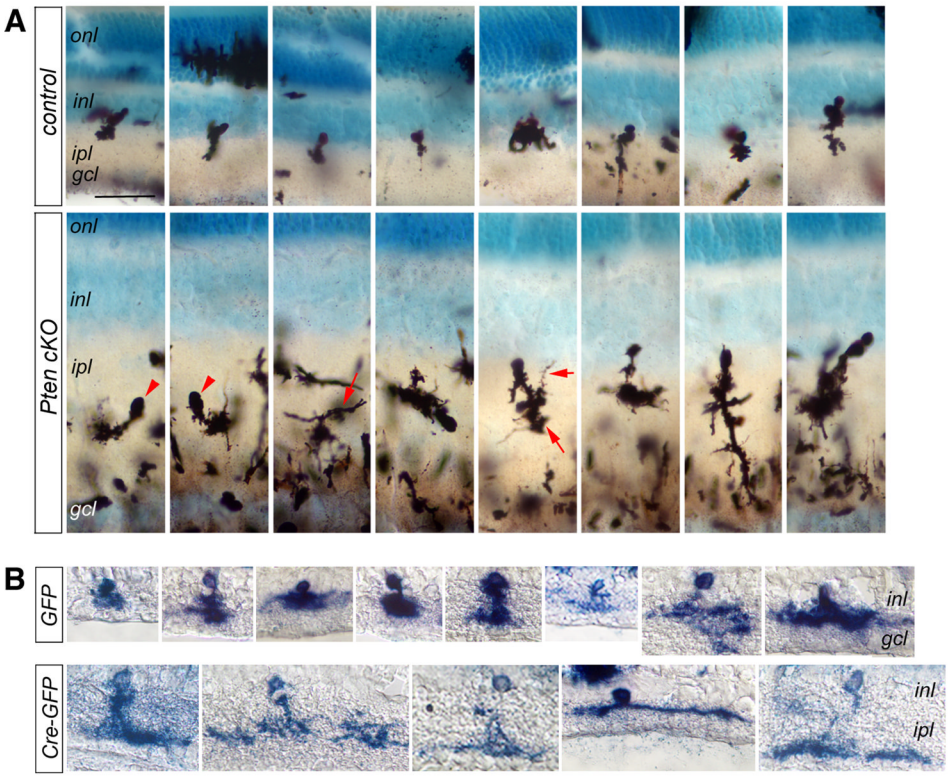

Figure 6. Pten deficiency causes abnormal arborization of amacrine interneurons

(A) Golgi staining of P45 control (top row) and *Pten* cKO (bottom row) retinas. Positive stained mutant cells show either Arrowheads point to abnormally positioned cell soma. Arrows indicate overly elaborate dendrites.

(B) Alkaline phosphatase histochemical labeling of individual transfected $Pten^{fl/fl}$ retinal cells at P21. $Pten^{fl/fl}$ retinas were electroporated with the control (LIA and GFP, top row) or cre-expressing (LIA, GFP and cre, bottom row) at P0 in vivo. Cre-expressing DNA transfected amacrine cells show more elaborate dendritic morphology.

gcl, ganglion cell layer; *inl*, inner nuclear layer; *ipl*, inner plexiform layer; *onl*, outer nuclear layer. Scale bar, A for (A, B), 40 μm.

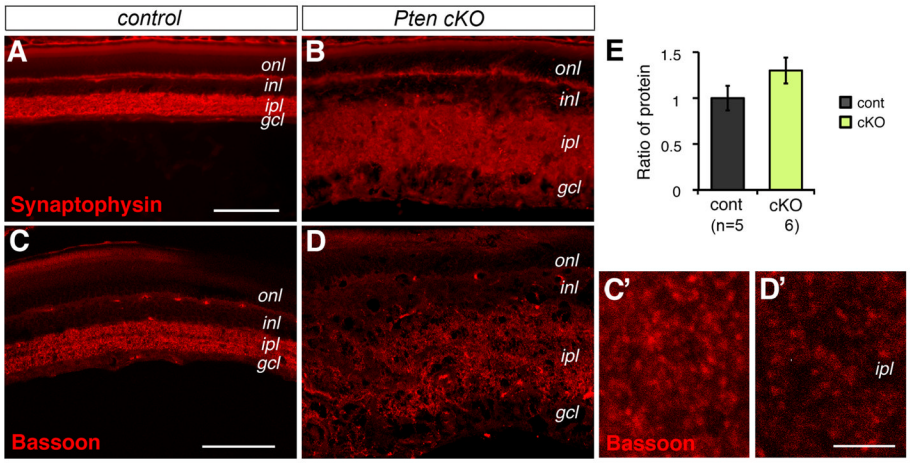

Figure 7. Pten mutant retina permits synaptogenesis in the inner plexiform layer

(A–D) Confocal images of immunolabeled control (A, C) and *Pten* cKO (B, D) retinas at P18 with synaptic markers Synaptophysin (A, B) and presynatic protein Bassoon (C, D). (C′, D′) show higher magnification images of the inner plexiform layer. *Pten* mutant retinas show the presence of Basson-labeled synaptic densities.

(E) Quantification of bassoon protein by Western blots at P18 did not detect significant change of total Bassoon protein levels (Individual retinas analyze (n) are indicated below the bar graphs. Mean ± S.E.M.

gcl, ganglion cell layer; *inl*, inner nuclear layer; *ipl*, inner plexiform layer; *onl*, outer nuclear layer. Scale bars, A for (A, B), 100 μm; C for (C, D), 75 μm; C′ for (C′, D′), 5 μm.

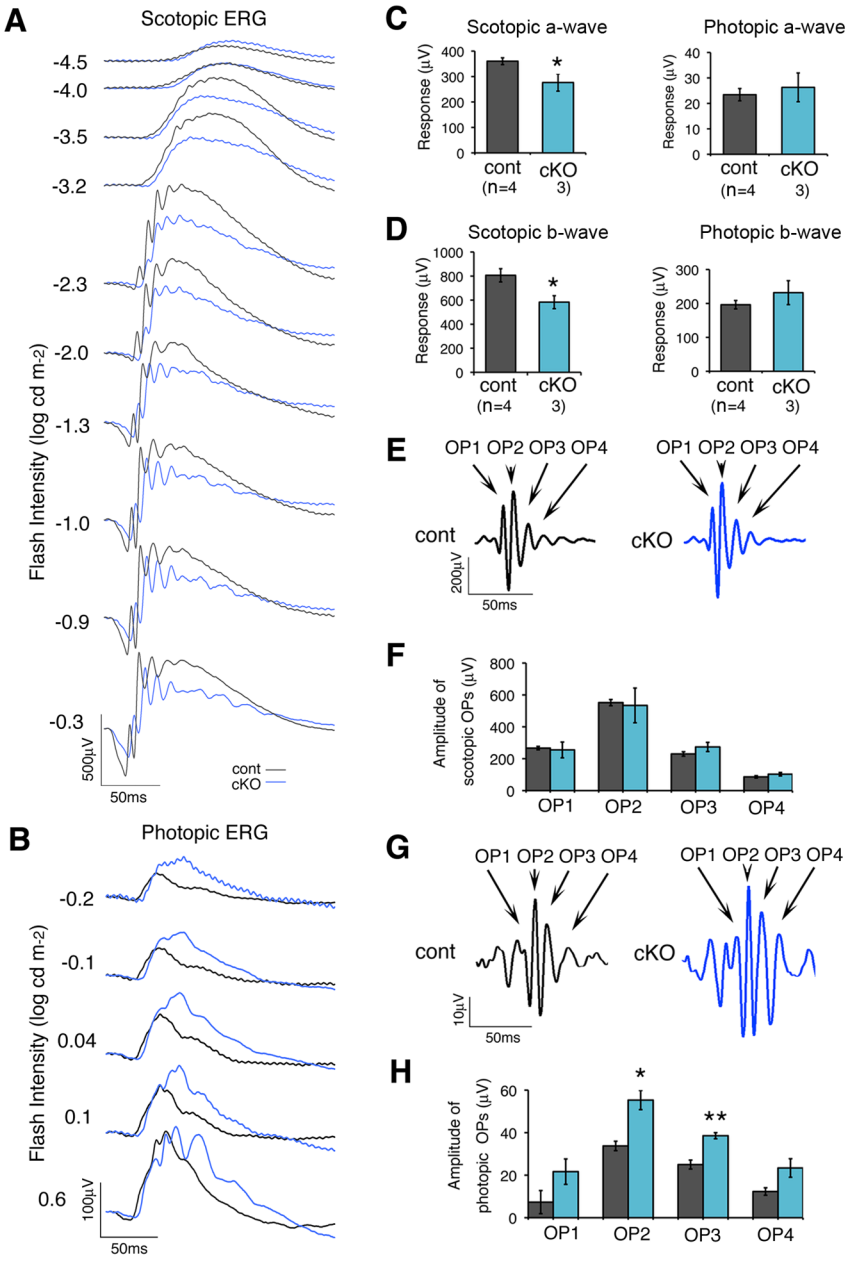

Figure 8. Pten deletion disrupts proper retinal function

(A, B) Representative scotopic (A) and photopic (B) ERGs at different light intensities from control (black trace) and *Pten* mutant (blue trace) mice.

(C, D) Amplitudes of a-wave (C) and b-wave (D) for scotopic and photopic ERGs. *Pten* mutants show significantly decreased scotopic a-wave and b-wave amplitudes (Individual animals tested (n) are indicated. Mean ± S.E.M. *, $p<0.05$).

(E–H) Comparison of oscillatory potential waveforms and amplitudes. *Pten* mutants show similar OPs as controls under dark-adapted conditions (E, F), but enhanced OP amplitudes after light adaptation (G, H) (Individual animals tested (n) are indicated. Mean ± S.E.M. **, $p<0.01$; *, $p<0.05$).

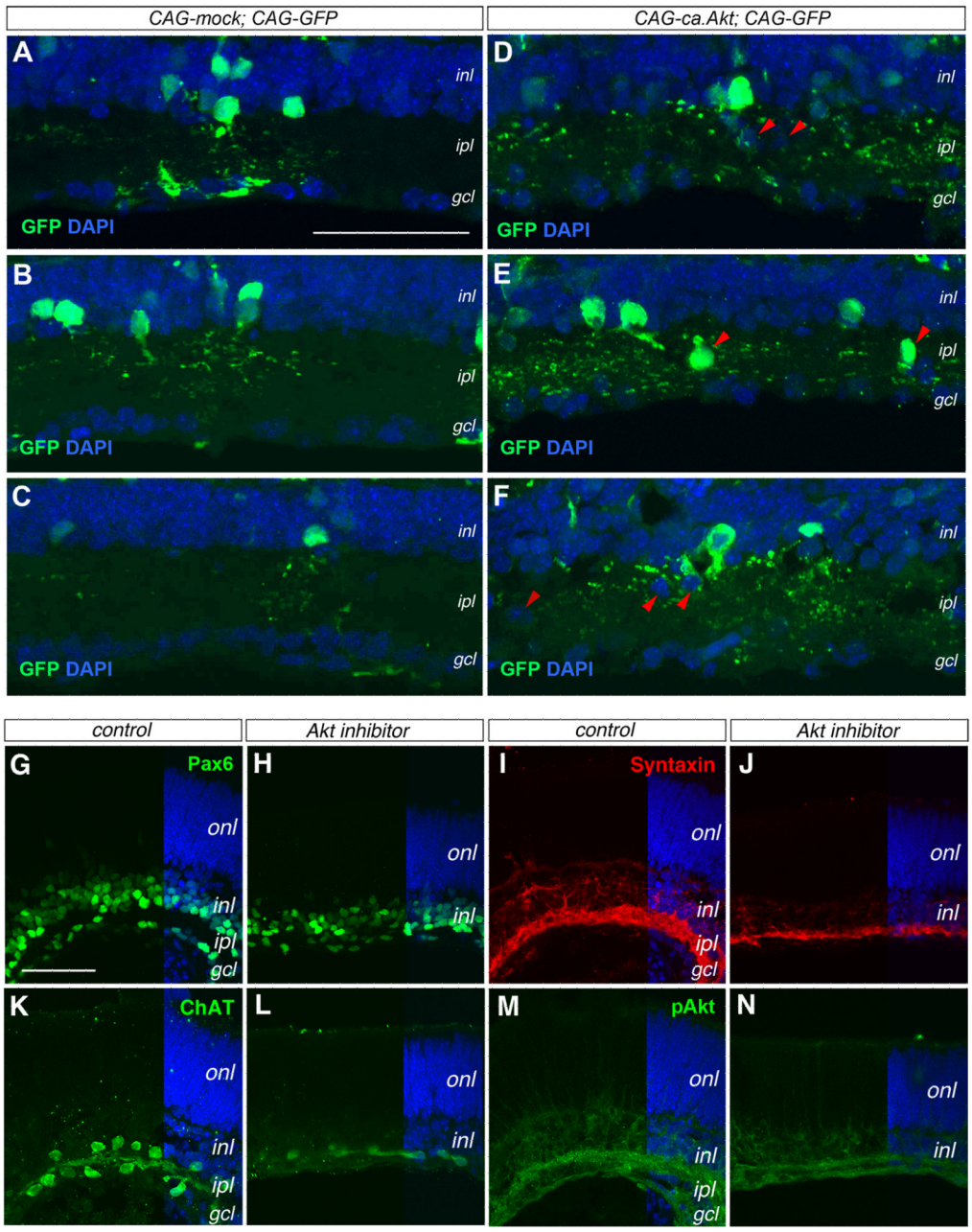

Figure 9. Akt activity affects amacrine cell morphogenesis and synaptic layer formation

(A–F) Effects of constitutively active Akt by immunolabeling for GFP (merged confocal images 10 μm). P21 wild type retinas electroporated in vivo at P0 with control CAG-mock and CAG-GFP DNAs (A–C) or CAG-ca,Akt and CAG-GFP DNAs (D–E). Panels (A–C) and (D–F) contain similar numbers of GFP+ cells, but (D–F) show >3 fold more GFP+ dendritic labeling in the *ipl*. The red arrowheads in (D–F) point to ectopically localized cell somata.

(G–N) Impacts of Akt inhibitor on inner plexiform layer formation. Confocal images of P0 retinal explants cultured without (G, I, K, M) or with Akt inhibitor (H, J, L, N) for 8 days are immunolabeled for Pax6 (G, H), Syntaxin (I, J), ChAT (K, L), and pAkt (M, N). *gcl*,

ganglion cell layer; *inl*, inner nuclear layer; *ipl*, inner plexiform layer; *onl*, outer nuclear layer. Scale bars, A for (A–F), G for (G–N), 50 μm.